Parameter selection method and performance assessment for the preliminary design of electrically powered transitioning VTOL UAVs

B. Theys* and J. De Schutter
KU Leuven, Leuven, Belgium

ABSTRACT

This paper describes a parameter selection method and performance assessment for the preliminary design of Vertical Take-Off and Landing Unmanned Aerial Vehicles (VTOL UAVs) that use a combination of wings and a set of electrically powered propellers for providing lift and thrust during cruise flight. This method allows us to quickly evaluate the possibilities of current technology for a given set of user and mission-specific requirements, and to create a preliminary design to meet these requirements. To this end, the acceptable range for the variable design parameters is predetermined and the parameters to optimize are identified. Mass and power models are presented for the components of the UAV and a novel model for a propeller in oblique flow conditions is applied. The models are used in a design algorithm that calculates all combinations of components. All feasible solutions are selected and displayed to the user after which the optimal solution can be chosen. A design case is presented and a sensitivity analysis shows the influence of different design parameters on this case.

1 INTRODUCTION

Currently, UAVs are increasingly deployed in various applications such as surveillance, mapping, inspection or transportation. VTOL UAVs such as multi-rotors prove to be advantageous over conventional fixed-wing UAVs due to their ability to land and take-off vertically or hover. The disadvantage is their limited flight speed and range. Therefore, VTOL UAVs are being developed that can transition from hover to efficient forward flight. Figure 1 presents two of such UAVs. A broad overview of hybrid UAV designs, their modelling and used control strategies, is presented by Saeed et. al. [1].

With improved performance, new applications or missions become possible, if a UAV can be designed that meets the mission-specific requirements. In many cases the user has only vague or conflicting requirements, since it is unknown whether these requirements are feasible or not. Therefore, a tool is required that can guide the user in defining the requirements by providing an overview of what is possible with current technology. A preliminary design that meets the requirements of the user is selected and presented as a set of design parameters with the associated performance.

Figure 1: Left: VertiKUL 1, designed to make a transition of 90° with a large wing to provide all the lift. Right: VertiKUL 2, designed to make a transition of 45° with smaller wings to improve wind gust resistance.

The design of a UAV consists of various systems and components with strong interactions. Multiple disciplines including propulsion, aerodynamics and materials are combined. The challenge for such integrated design is to capture interactions between the various systems and components. In recent years, multiple integrated design environments have been developed by industrial, governmental, and academic research groups [2]. A good example of an integrated design environment is the Boeing Integrated Vehicle Development System (BIVDS) [3] for the development of various types of aircraft. For multi-rotor UAVs, the optimal selection of propulsion components is addressed in [4]. In this work, payload, number of rotors and flight duration is fixed. Other studies on automated design methods for multi-rotor UAVs are described by Bouabdallah [5] and Lundstrom [6]. Lundstrom goes a step further than preliminary design; the CAD files are subsequently evaluated with a panel code for detailed aerodynamic evaluation. Aksugur [7] presents a design methodology, specifically for tailsitter UAV concepts with a hybrid propulsion system based on analytical calculations and experimental data.

From a general engineering point of view, the design process of a new product is split into several phases [8]. The present paper focusses on the first two phases: feasibility

*Email address: bart.theys@kuleuven.be

study and preliminary design. The goal of the parameter selection method in the presented paper is to have absolute freedom in specifying which of the design parameters are varied to come to an optimal solution and to have a flexible tool to evaluate the possibilities of current technology. Feasible preliminary designs are generated within a weight class and type or family of UAV that use a similar design approach. The incentive for the development of this parameter selection method originated from the design of a VTOL UAV for autonomous parcel delivery, presented in [9]. In this prior work, a more dedicated design method is presented for a case in which many of the design parameters had already been fixed [10], reducing the size of the parameter space.

Section 2 models the systems and components that are used for an electrically powered multi-rotor VTOL UAV. Next, section 3 describes the algorithm that evaluates all possible designs and presents the best solution, based on a set of user requirements. Finally, the design process is demonstrated for a specific case and the impact of technology on the performance of the design is discussed in section 4.

2 COMPONENT MODELLING

An electrically powered multi-rotor VTOL UAV consists of many components. Components that are not decided in advance can be modelled using three different methods. A statistical method models a component based on data from existing components. It therefore requires a dataset that is both dense enough to provide a high accuracy and large enough to cover a broad range of designs, since extrapolating these models can lead to erroneous results. An analytical or quasi-analytical method models components based on their underlying physical properties and behaviour. This method allows us to extrapolate and requires only little data of existing components to validate the model. However, this data needs to be representative for the design problem and the accuracy might be low. Finally, a design-based method is an accurate method based on component-specific parameters that determine directly the properties of the component. However, not many UAV components can be modelled with this method.

All three methods are used for the component modelling described in the present paper. This section provides general models for the different components that contribute to the mass and performance of the UAV: body, wing, propellers, motor, electronic speed controller (ESC) and battery. The accuracy of the design algorithm is only as accurate as the models of these components. Individual models can be easily updated if new technology becomes available.

2.1 Body and wing

The aerodynamic performance of the design consists of the drag of the UAV without wings, D_{body}, and the lift and drag of the wings, L_{wing} and D_{wing}, that can be added to the UAV. As it is common practice in helicopter performance identification [11], the drag of the UAV without lifting surfaces is modelled by an equivalent frontal surface A_{eq} with $C_D = 1$:

$$D_{body} = \frac{1}{2} V^2 \rho \, A_{eq}, \tag{1}$$

with V the speed and ρ the air density. The drag of the wing is assumed to have a parabolic relationship with the lift coefficient and is calculated as:

$$D_{wing} = \frac{1}{2} C_{D_{wing}} V^2 \rho \, A_{wing}. \tag{2}$$

With

$$C_{D_{wing}} = C_{D0} + \frac{C_L^2}{\pi \, AR \, e}. \tag{3}$$

Herein, C_{D0} represents the drag coefficient of the airfoil at zero-lift. The aspect ratio of the wing AR is defined as $AR = \frac{b^2}{A_{wing}}$ with b the span of the wing and A_{wing} the wing surface area. The span efficiency factor e can vary between 0.65 and 0.93 [12]. The lift coefficient of the finite wing, C_L, is calculated based on the zero-lift angle, α_0, and the lift slope of the finite wing a_{wing}, which is smaller than the lift slope of the airfoil, a_0.

$$C_L = a_{wing}(\alpha_{wing} - \alpha_0), \tag{4}$$

with the lift slope for a finite wing calculated as:

$$a_{wing} = \frac{a_0}{1 + \frac{a_0}{\pi \, AR \, e}}. \tag{5}$$

The mass of the body m_{body} depends on many factors such as the size, total mass m_{tot} and thrust-to-weight ratio of the UAV, the materials used and quality of the construction method. In this paper the mass of the body is modelled with a quasi-analytical method as a fraction k_{body} of the total mass:

$$m_{body} = k_{body} \, m_{tot}. \tag{6}$$

Since wings can be added to the body, their mass can be modelled separately. The mass of the wing consists of surface material that covers the wing, $m_{surface}$, core material to shape the wing, m_{core}, and a central beam with mass m_{beam} to increase stiffness and strength.

$$m_{wing} = m_{surface} + m_{core} + m_{beam} \tag{7}$$

Figure 2 illustrates these different components for a lightweight UAV wing. An accurate design-based method is used for the surface and core material:

$$m_{surface} = 2 \, k_{surface} \, A_{wing} \tag{8}$$

$$m_{core} = k_{core} \, V_{wing} \tag{9}$$

with V_{wing} the volume of the wing, $k_{surface}$ the area density of the surface material and k_{core} the volumetric mass density of the core material.

The mass of the central beam is modelled with an analytical method that is based on the use of a hollow, thin-walled

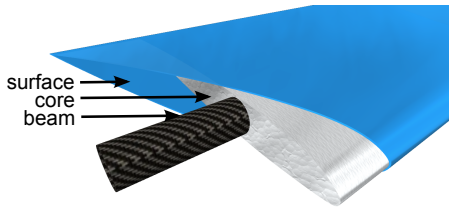

Figure 2: Lightweight construction of a UAV wing.

cylindrical tube. A maximum allowed deflection of the tip of the beam in the lateral direction, x, relative to the span of the wing is imposed to guarantee the stiffness of the wing $x_{rel} = \frac{x}{b/2}$. The relative deflection of the beam with one end clamped and the load $q = \frac{m_{tot}\, G\, g}{b}$ assumed to be equally distributed, is calculated as:

$$x_{rel} = \frac{q\,(b/2)^3}{8\,I\,E} \tag{10}$$

Herein is G the load factor and E the Young's modulus of the material of the beam. The area moment of inertia is calculated as $I = \pi\,(d/2)^3\,t_{beam}$, with d the thickness of the wing thus maximum diameter of the beam and t_{beam} the wall thickness of the beam. The thickness of the wing is calculated as $d = c\,t_{af}$ with c the chord of the wing and t_{af} the maximum relative thickness of the selected airfoil. We can now calculate the required thickness of the beam as:

$$t_{beam} = \frac{m_{tot}\, G\, g\, b^2}{8\,\pi\,E\,c^3\,t_{af}^3\,x_{rel}} \tag{11}$$

The mass of the beam m_{beam} is calculated as:

$$m_{beam} = \frac{m_{tot}\, G\, g\, b^3}{8\,E\,c^2\,t_{af}^2\,x_{rel}} = k_{beam}\,\frac{m_{tot}\, G\, g\, b^3}{c^2}. \tag{12}$$

The constant k_{beam} can be experimentally determined or calculated as

$$k_{beam} = (8\,E\,t_{af}^2\,x_{rel})^{-1} \tag{13}$$

Comparable models are presented by Noth [13], Tennekes [14] and Rizzo & Frediani [15].

2.2 *Propellers*

The propeller model presented in this paper goes one step further than most propeller models. Usually for multi-rotor UAVs, the propeller is modelled in near-hover conditions. For a transitioning UAV, however, the propeller will travel through the air at high speeds and angles α_{plr} ranging from $0°$ to $90°$ [16] as illustrated on figure 3 with F_{plr} the force vector produced by the propeller and α_{plr} defined as the angle of the propeller with respect to the free-stream airspeed. For a propeller with a specified diameter, momentum theory provides an expression for the consumed 'ideal' power. Glauert [17] generalized the axial momentum theory from Rankine - Froude [18] for a propeller operating in oblique flow:

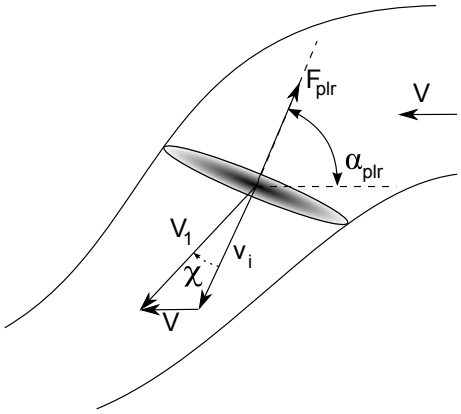

Figure 3: A propeller in oblique flow.

$$V_1 = \sqrt{(V\sin\alpha_{plr})^2 + (V\cos\alpha_{plr} + v_i)^2} \tag{14}$$

$$F_{plr} = 2\rho A_{plr} v_i V_1 \tag{15}$$

$$P_i = F_{plr}(v_i + V\cos\alpha_{plr}) \tag{16}$$

$$P_{mech} = \frac{P_i}{\eta_{plr}} \tag{17}$$

Herein is V_1 the airspeed vector at the propeller, v_i the propeller induced velocity and A_{plr} the propeller disk area. Equations (14) to (17) allow to calculate the required mechanical power P_{mech} if the propeller efficiency η_{plr} is known. From wind tunnel tests of a propeller in oblique flow conditions [16], it was found that the propeller efficiency decreases for an increasing skewing angle χ, that is calculated as:

$$\chi = \tan^{-1}\left(\frac{V\sin(\alpha_{plr})}{(v_i + V\sin(\alpha_{plr}))}\right) \tag{18}$$

A correlation between the propeller efficiency in hover $\eta_{plr_{hover}}$ and skewing angle was found [19]:

$$\eta_{plr} = \frac{\eta_{plr_{hover}}}{4.1\cdot 10^{-6}\chi^3 - 0.00028\chi^2 + 0.006\chi + 1} \tag{19}$$

With χ expressed in degrees. This correlation takes into account the loss in efficiency due to the off-design working regime of the propeller.

The mass of the propeller m_{plr} is modelled as recommended by the 'General Dynamics propeller weight method' described by Roskam [20] for plastic or composite propellers:

$$m_{plr} = k_{plr}\, n_{blades}^{k_{blades}}\,(D_{plr}\, P_{mech_{max}})^{e_{plr}} \tag{20}$$

With n_{blades} the number of blades, D_{plr} the diameter of the propeller, $P_{mech_{max}}$ the maximum mechanical power that the motor delivers to the propeller and k_{plr}, k_{blades} and e_{plr} model-specific values.

2.3 Battery - motor - ESC

In this paper, the battery is characterized solely by its mass m_{bat} and energy E_{bat}. Although the volume of the battery can also be a limiting factor in some designs, for UAVs usually the mass is more important. For the study in this paper we therefore propose following design-based model [21]:

$$E_{bat} = k_{bat}\, m_{bat}\, f_{usable} \tag{21}$$

Herein is f_{usable} (< 1) the fraction of the total energy of the battery that will be consumed each cycle in order to extend lifetime of the battery. Many chemistries of battery are possible to use for electrically powered UAVs. Therefore, the battery mass constant k_{bat} has to be adapted for the selected type of battery.

The motor is modelled with a statistical method as a component with a mass m_{mot} and a maximum rated power, $P_{mot_{max}}$.

$$m_{mot} = k_{mot} P_{mot_{max}}, \tag{22}$$

with the motor mass constant k_{mot} determined in a statistical way from a large data set of existing motors [21]. The efficiency of the conversion to mechanical energy from electrical energy of the motor is determined by:

$$P_{mech} = \eta_{mot}\, P_{ele} \tag{23}$$

The electronic speed controller (ESC) is modelled similarly as the motor with k_{ESC} the mass constant and η_{ESC} the efficiency.

3 Design algorithm

3.1 Parameter classification

A preliminary design is defined by a large set of parameters that have mutual interactions and cannot all be changed independently of each other. A limited set with the most important parameters is selected to be used in the design algorithm to keep the calculation time as low as possible. As input parameters for one design, a minimum set of parameters that define one design is selected so that remaining output parameters can be determined by straightforward calculations that require only a very small computational time. The input parameters are divided into fixed parameters and iteration parameters. The fixed parameters, for example gravity g or mass of the avionics m_{av}, are kept constant throughout one run of the algorithm. The iteration parameters are the parameters for which the user does not yet know what value to select in order to find a design that meets the requirements such as for example total mass m_{tot}, battery mass m_{bat}, propeller diameter D_{plr}, ... Output parameters are calculated based on the component models and their mutual relations. The user applies the desired boundaries to these parameters, such as minimum required speed, maximum allowed span, minimum required range, ... Figure 4 presents a schematic overview of the classification of the set of parameters. In this figure, the parameters in the shaded region of the input parameter space are iterated and on the parameters in the shaded region of the output parameter space, boundaries are applied. Input parameters outside the shaded region are decided in advance or cannot be changed by the user. Output parameters outside the shaded region are parameters that are calculated, but that are not of any interest to the user.

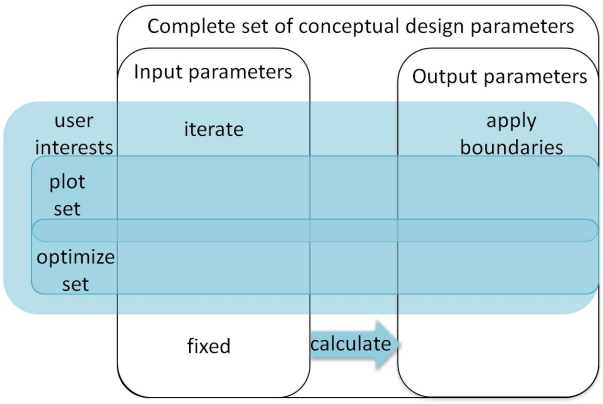

Figure 4: Schematic presentation of the parameter classification.

Table 1 presents the set of input parameters with their valid range that are used to calculate remaining output parameters.

3.2 Calculation method

Based on the selected set of input parameters, the remaining output parameters are calculated. First the aerodynamic properties of the UAV are calculated following equation (1) to (3). Next, the cruise flight speed is calculated. Based on the assumption that the UAV flies at a constant speed and altitude with the geometry determined by the input parameters, only one flight speed results in a force equilibrium, illustrated in figure 5:

$$F_{prop} = F_{plr} n_{plr} \tag{24}$$

Herein is n_{prop} the number of propellers.

$$L_{prop} = F_{prop} \sin \alpha_{prop} \tag{25}$$

$$T_{prop} = F_{prop} \cos \alpha_{plr} \tag{26}$$

$$T_{prop} = D = \frac{1}{2} \rho V_{cruise}^2 (A_{eq} + A_{wing} C_{D_{wing}}) \tag{27}$$

$$L_{prop} = T_{prop} \tan \alpha_{plr} \tag{28}$$

$$L_{wing} = \frac{1}{2} \rho V_{cruise}^2 A_{wing} C_{L_{wing}} \tag{29}$$

$$L_{prop} + L_{wing} = m_{tot}\, g \tag{30}$$

$$V_{cruise}^2 = \frac{2\, m_{tot}\, g}{\rho \Big(\tan \alpha_{plr} (A_{eq} + A_{wing} C_{D_{wing}}) + A_{wing} C_{L_{wing}} \Big)} \tag{31}$$

Symbol	explanation	value	unit
D_{plr}	propeller diameter	$0.1 - 0.6$	$[m]$
$C_{L_{wing}}$	wing lift coefficient	$0.1 - 1.2$	$[-]$
m_{tot}	total mass	$1 - 10$	$[kg]$
α_{plr}	propeller angle	$0 - 90$	$[°]$
n_{prop}	number of propellers	$4 - 8$	$[-]$
A_{wing}	wing surface	$0 - 1$	$[m^2]$
mf_{bat}	battery fraction	$0.1 - 0.8$	$[-]$
dim_{dia}	max. dimension	$0.4 - 2$	$[m]$
m_{av}	avionics mass	0.12	$[kg]$
P_{av}	avionics power	1	$[W]$
P_{pld}	payload power	0	$[W]$
$t_{rel_{hover}}$	rel. time in hover	0.05	$[-]$
TW_{ratio}	thrust to weight	1.5	$[-]$
ρ	air density	1.22	$[kg/m^3]$
g	gravitation	9.81	$[m/s^2]$
k_{bat}	bat. energy density	$120 - 360$	$[Wh/kg]$
η_{esc}	ESC efficiency	0.95	$[-]$
η_{mot}	motor efficiency	0.75	$[-]$
k_{esc}	ESC mass cnst.	$1/10000$	$[kg/W]$
k_{mot}	motor mass cnst.	$1/3400$	$[kg/W]$
n_{blades}	number of plr blades	2	$[-]$
k_{plr}	propeller mass cnst.	$4.4 \cdot 10^{-4}$	$[-]$
k_{blades}	plr blade mass cnst.	0.391	$[-]$
e_{plr}	plr mass model exp.	0.782	$[-]$
$\eta_{plr_{hover}}$	plr hover efficiency	0.7	$[m]$
k_{drag}	drag cnst.	$0.1 - 0.25$	$[-]$
AR	Aspect Ratio	$1 - 10$	$[-]$
e	Oswald factor	0.85	$[-]$
C_{d0}	Zero-lift drag	0.01	$[-]$
a_0	airfoil lift slope	2π	$[-/rad]$
k_{body}	body structure quality	$0.1 - 0.2$	$[-]$
k_{beam}	wing structure quality	0.014	$[m^2/s^2]$
$k_{surface}$	surface mass cnst.	$0.05 - 0.35$	$[kg/m^2]$
k_{core}	wing core mass cnst.	$10 - 40$	$[kg/m^3]$
f_{usable}	usable bat. capacity	0.8	$[-]$

Table 1: Used set of preliminary design input parameters.

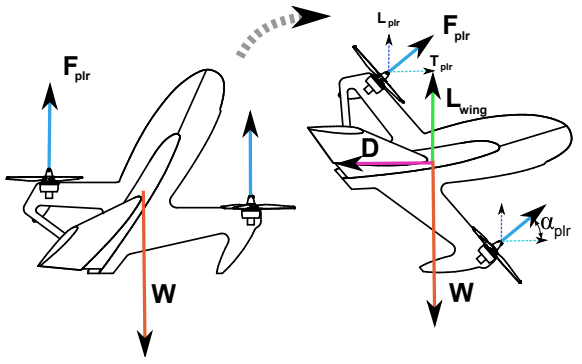

Figure 5: Overview of the forces acting upon a transitioning UAV in hover and in cruise flight.

With the speed known, the required mechanical power for the propulsion system in cruise flight is calculated with equations (14) to (17). Next, the mechanical power is also calculated for hover and maximum throttle regime and the electrical power for one propulsion system P_{ele} is calculated with equation (23). The mass of the propulsion system results from the maximum required power and is calculated with the models, presented in section 2. The total electrical power consumption P_{tot} is found by:

$$P_{tot} = P_{prop} + P_{av} + P_{pld} \tag{32}$$

In which the power of the avionics P_{av} and the power of the payload P_{pld} is known. The power of the propulsion system P_{prop} is calculated as:

$$P_{prop} = n_{prop}\, P_{ele}. \tag{33}$$

The mass of the structure and wings is calculated with equations (6) to (12) and the remaining mass available for payload is found by:

$$m_{pld} = m_{tot} - m_{av} - m_{body} - m_{prop} - m_{wing} - m_{bat} \tag{34}$$

Note that this formula can result in a negative payload mass for a set of input parameters; these solutions are filtered out by the boundary condition of a minimum payload mass that is above $0\ kg$. The total flight time is:

$$t_{flight_{total}} = \frac{E_{bat}}{((1 - t_{rel_{hover}})P_{tot_{cruise}} + t_{rel_{hover}} P_{tot_{hover}}}. \tag{35}$$

Herein is $t_{rel_{hover}}$ the relative amount of mission time spend in the hover phase and $P_{tot_{cruise}}$ and $P_{tot_{hover}}$ are calculated with equation (33) for cruise and hover phase respectively. The flight time in cruise is

$$t_{flight_{cruise}} = t_{flight_{total}}(1 - t_{rel_{hover}}). \tag{36}$$

Therefore, the range of the UAV is

$$d = t_{flight_{cruise}}(V_{cruise} - V_{wind}), \tag{37}$$

with V_{wind} the headwind during flight and V_{cruise} as in equation (31).

3.3 Algorithm work flow

The whole parameter space that is defined by the iteration input parameters, is evaluated in order to find the global optimum that is specified by the mission requirements. For each combination of the iteration input parameters in combination with the fixed input parameters, the remaining parameters of the preliminary design are calculated. Afterwards, the designs are filtered to only keep solutions that lie within the parameter space, defined by boundaries set by the user. The parameters of interest from the set of solutions are then plotted on 2D or 3D graphs to give the user an overview of the

trade-offs between these parameters. This is useful in case the user wants to optimize more than one parameter like for instance both speed and range. Instead of choosing the design that meets the user requirements and performs best in terms of parameters to optimize, weights can be applied to the set of parameters to optimize and the best solution can be computed from the valid solution set. This best solution, based on weights applied to parameters to optimize, is highlighted in the plots that present all solutions. The design algorithm is schematically presented in figure 6.

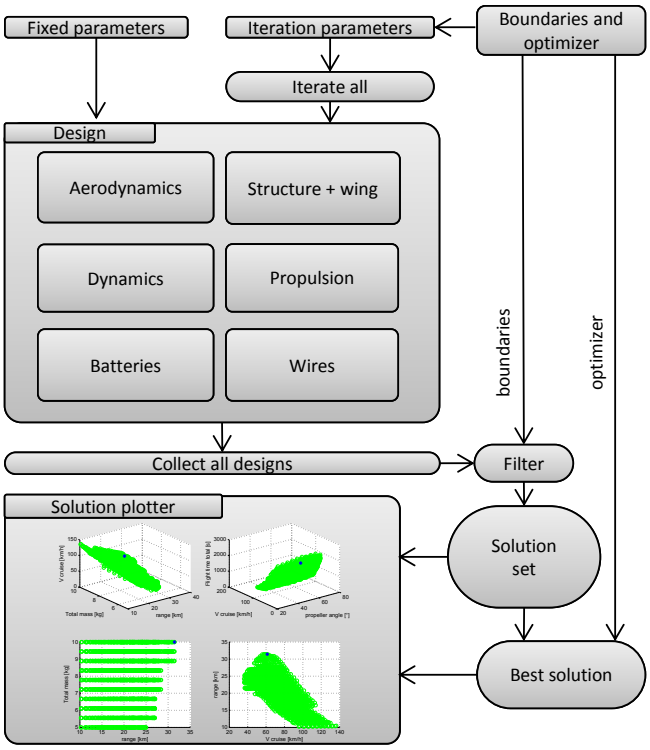

Figure 6: Overview of the design algorithm.

The set of design parameters is stored in a spreadsheet and forms the basis for a parametric CAD model.

4 Design Case

As a demonstration of the algorithm, this section presents a case for which a UAV has to transport a package of $1kg$ as far and as fast as possible. The total mass should not exceed $5kg$ and the span should not exceed $0.8m$. The input parameters are chosen according to table 1, except for those specified in particular for this mission and presented in table 2.

The algorithm now calculates the performance for a set of 15000 combinations of input parameters. On figure 7, all dots present possible solutions. The best solutions in terms of speed and range lie on the right top edge of the solution cloud on the right graph. From this graph, the user selects the preferred performance. The user can observe that there is no point in flying slower than $14m/s$, since both range and speed will decrease. Above this speed, the user needs to make a trade-off between speed and range. In this case we select a UAV design with a range of $33.4km$ and a cruise speed of $16.3m/s$, marked with the star on the graphs. Figure 8 shows the mass distribution of the selected design with a total mass of $5kg$. Battery and payload represent almost two third of the total mass.

Parameter	type	value	unit
D_{plr}	iterate 3	$0.229 - 0.279$	$[m]$
$C_{L_{wing}}$	iterate 5	$0.1 - 1.2$	$[-]$
A_{wing}	iterate 5	$0 - 0.2$	$[m^2]$
mf_{bat}	iterate 10	$0.3 - 0.6$	$[-]$
α_{plr}	iterate 20	$0 - 80$	$[^\circ]$
m_{tot}	fixed	5	$[kg]$
n_{prop}	fixed	4	$[-]$
dim_{dia}	fixed	0.8	$[m]$
k_{bat}	fixed	220	$[Wh/kg]$
k_{drag}	fixed	0.1	$[-]$
AR	fixed	2	$[-]$
k_{body}	fixed	0.15	$[-]$
$k_{surface}$	fixed	0.05	$[kg/m^2]$
k_{core}	fixed	10	$[kg/m^3]$
f_{usable}	fixed	0.8	$[-]$
$t_{flight_{tot}}$	boundary	$0 - \infty$	$[s]$
m_{pld}	boundary	$1 - \infty$	$[kg]$
V_{cruise}	boundary & optimize	$0 - \infty$	$[m/s]$
$range$	boundary & optimize	$0 - \infty$	$[m]$

Table 2: Mission specific parameters for the design case.

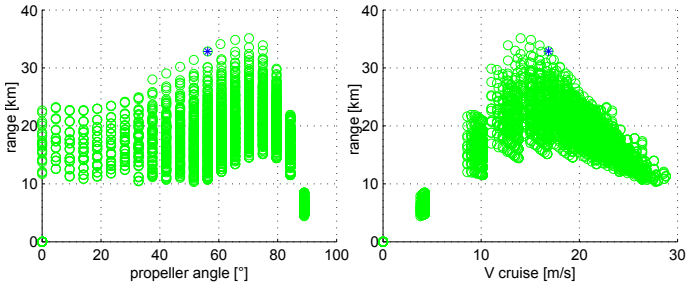

Figure 7: Set of 2895 feasible solutions resulting from one run of the algorithm, with the chosen solution highlighted.

4.1 *Off-Design performance*

Now that the preliminary design is fixed, the performance of the UAV in other flight regimes can be evaluated. To this end, the transition angle is varied from hover up to the point for which the propulsion system delivers its maximum rated power; this is the top speed. Lift and drag of the UAV are calculated for each transition angle with equations (2) and (4) and the speed and associated power are calculated according to equations (31) and (32). The simulated performance of the

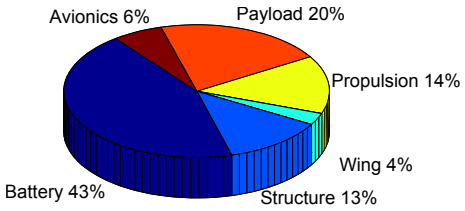

Figure 8: Mass distribution of the selected design.

selected design is plotted in figure 9. The graphs in this figure show that the required power drops significantly from hover up to $10m/s$, which is due to two reasons. The first reason is the more energy efficient working regime of the propellers due to the speed of the incoming air stream. The second reason is the beneficial effect of the added wing, that becomes more pronounced at higher speeds and angles of attack that approach the design point. The highest range is achieved at about $13.5m/s$, this is lower than the selected design speed of $16.3m/s$, since a trade-off was made between speed and range. The longest flight time is achieved at an even slower speed of only $10m/s$, the point at which power consumption is the lowest.

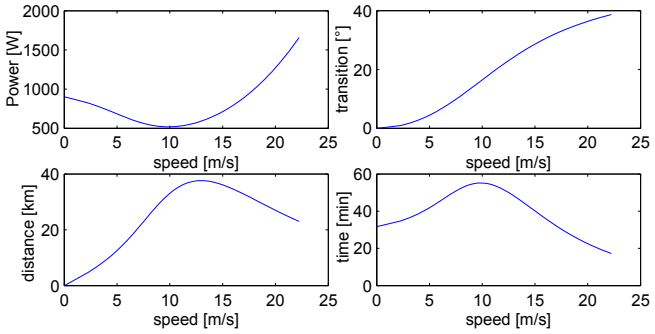

Figure 9: Simulated performance of the chosen design from hover to maximum speed.

4.2 Parametric sensitivity analysis

On the one hand, the parameter selection method allows to quickly evaluate the impact of technology improvements on the performance of electrically powered multi-rotor VTOL UAVs. An improvement in technology translates into an updated model for the different components, described in section 2. On the other hand, the parameter selection method is flexible in a way that the user can choose to broaden or narrow the parameter space, to evaluate the influence of these boundaries on the best performing design. As an example, the impact of technology and the influence of the user selected boundaries on the performance of the selected design in terms of speed and range are graphically presented in figure 10 for a select set of design parameters. The bars on this chart present the relative impact of a 10% change of these parameters on respectively the possible speed and range of the presented design.

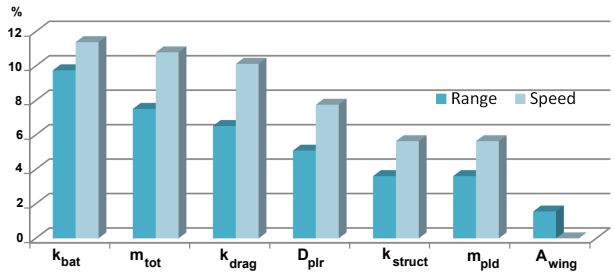

Figure 10: Relative influence of different design parameters on the best performing solution in terms of range and speed.

This analysis learns that for the design case in this paper, the energy density of the battery has the largest impact on the range and speed of the design. It also becomes clear that increasing the allowed total mass m_{tot} of $5kg$ or increasing the maximum allowed propeller diameter, has a large impact on the performance of the design. After the battery energy density and the total mass, decreasing the drag of the body of the UAV is most important in achieving higher range or speed. Increasing the allowed wing surface for this design did not have any influence on increasing the speed, but did have a small influence on increasing the range. It should be noted that this sensitivity analysis is only valid for the design case presented in this paper.

5 Conclusion

This paper presented a parameter selection method for the preliminary design and performance assessment of electrically powered multi-rotor VTOL UAVs. The method makes use of simplified models for the different components of the UAV. A novel propeller model is introduced, which takes into account the beneficial effect of an incoming air velocity at oblique flow conditions and efficiency losses due to the off-design working conditions. The performance of all possible design combinations of a user defined input parameter space is calculated and evaluated. The advantages of this approach are that the global optimum of the input set is always found and that the tool is flexible in a way that the user can choose the range of the parameters, the iteration resolution and the parameters to optimize. The disadvantage is the vast increase in computing time when the input parameter space is enlarged by increasing the resolution or increasing the range of the parameters. A solution to reduce computing time, is evaluating a broad range of input parameters with a low resolution and zooming in around the best solution during a second run of the algorithm to increase the resolution. The design algorithm provides a tool to evaluate the possibilities with the current technology and serves as initial sizing and component selection for all types of missions for VTOL UAVs. To improve the accuracy of the parameter selection method, more detail can be added to the individual models or more statistical models

can be used. Therefore, a large and detailed database of different components is required. Flight tests on existing UAVs and prototypes can be used to validate the method and refine the models for the aerodynamics of wing, body and propeller, since these can only be measured in flight or in wind tunnel experiments. After creating a preliminary design with this method, a parametric CAD model can be generated and high-fidelity modelling such as finite element modelling can be used for the detailed design of the UAV.

REFERENCES

[1] Adnan S Saeed, Ahmad Bani Younes, Shafiqul Islam, Jorge Dias, Lakmal Seneviratne, and Guowei Cai. A review on the platform design, dynamic modeling and control of hybrid uavs. In *Unmanned Aircraft Systems (ICUAS), 2015 International Conference on*, pages 806–815. IEEE, 2015.

[2] Kevin G Bowcutt. A perspective on the future of aerospace vehicle design. *AIAA Paper*, 6957:2003, 2003.

[3] Joel E Hirsh, Joseph B Wilkerson, and Robert P Narducci. An integrated approach to rotorcraft conceptual design. In *45th AIAA Aerospace Sciences Meeting and Exhibit*, pages 8–11, 2007.

[4] Christos Ampatis and Evangelos Papadopoulos. Parametric design and optimization of multi-rotor aerial vehicles. In *Applications of Mathematics and Informatics in Science and Engineering*, pages 1–25. Springer, 2014.

[5] S. Bouabdallah. *Design and control of quadrotors with application to autonomous flying*. Ph.D. dissertation, 2007.

[6] David Lundström, Kristian Amadori, and Petter Krus. Automation of design and prototyping of micro aerial vehicle. In *47th AIAA Aerospace Sciences Meeting and Exhibit, Orlando, FL, USA*, 2009.

[7] Mirac Aksugur and Gokhan Inalhan. Design methodology of a hybrid propulsion driven electric powered miniature tailsitter unmanned aerial vehicle. *Journal of Intelligent and Robotic Systems*, 57(1-4):505–529, 2010.

[8] Morris Asimow. *Introduction to design*, volume 394. Prentice-Hall Englewood Cliffs, NJ, 1962.

[9] Menno Hochstenbach, Cyriel Notteboom, Bart Theys, and Joris De Schutter. Design and control of an unmanned aerial vehicle for autonomous parcel delivery with transition from vertical take-off to forward flight-vertikul, a quadcopter tailsitter. *International Journal of Micro Air Vehicles*, 7(4):395–406, 2015.

[10] Menno Hochstenbach and Cyriel Notteboom. *Ontwerp en bouw van een onbemand vliegtuig voor autonoom pakkettransport met gecontroleerde transitie van verticaal opstijgen naar voorwaartse vlucht*. PhD thesis, Master Thesis, KU Leuven, 2014.

[11] Raymond W Prouty. *Helicopter performance, stability, and control*. 1995.

[12] Jan Roskam and Chuan-Tau Edward Lan. *Airplane aerodynamics and performance*. DARcorporation, 1997.

[13] Andre Noth, Roland Siegwart, and Walter Engel. *Design of solar powered airplanes for continuous flight*. PhD thesis, ETH, 2008.

[14] Hendrik Tennekes. *The simple science of flight: from insects to jumbo jets*. MIT press, 2009.

[15] E Rizzo and A Frediani. A model for solar powered aircraft preliminary design. *Aeronautical Journal*, 112(1128):57–78, 2008.

[16] Bart Theys, Gregorius Dimitriadis, Thomas Andrianne, Patrick Hendrick, and Joris De Schutter. Wind tunnel testing of a vtol mav propeller in tilted operating mode. In *Unmanned Aircraft Systems (ICUAS), 2014 International Conference on*, pages 1064–1072. IEEE, 2014.

[17] Hermann Glauert. Airplane propellers. In *Aerodynamic theory*, pages 169–360. Springer, 1935.

[18] W Froude. On the elementary relation between pitch, slip, and propulsive efficiency. 1920.

[19] B. Theys, G. Dimitriadis, P. Hendrick, and J. De Schutter. Experimental and numerical study of mini-uav propeller performance in oblique flow. *To appear in AIAA Journal of Aircraft*, 2016.

[20] J Roskam. Airplane design, part v: component weight estimation, 1985. *Roskam Aviation Corporation, Ottawa, Kansas*, page 85.

[21] Jay Gundlach. *Designing unmanned aircraft systems: A comprehensive approach*. American Institute of Aeronautics and Astronautics, 2012.